LIMIT ANALYSIS FOR PLANE STRESS PROBLEM BY USING NURBS BASED ON BÉZIER EXTRACTION IN COMBINATION WITH SECOND ORDER CONE PROGRAM

Do Van Hien, Ho Ngoc Bon, Van Huu Thinh
Ho Chi Minh City University of Technology and Education, Vietnam

Received 28/8/2018, Peer-reviewed 12/11/2018, Accepted for publication 22/11/2018

ABSTRACT

This paper presents a new approach to estimate limit load factor by using Non-Uniform Rational Basis Spline (NURBS) based on Bézier extraction in combination with Second-order Cone Programming (SOCP) for plane stress problem. This approach based on an upper bound method with rigid-perfectly plastic material model. A NURBS basis functions are used for both geometry and field approximation. Limit analysis problem is transformed into the form of a SOCP problem which can be solved by efficient primal-dual interior point algorithm. The numerical results show that the effectiveness and accuracy of the present approach by comparing its performance with other methods reported in the available literature. Based on the results, the present an approach is a promising tool for computing of structure limit analysis.

Keywords: *NURBS; IGA; Limit analysis; Bézier extraction; SOCP; Upper bound.*

1. INTRODUCTION

Nowadays, limit analysis is a key part of structural design and safety assessment of many engineering structures especially in nuclear power plants, chemical industry, metal forming and civil engineering. The most important outcomes of a structural limit analysis is a limit factor. It is useful for the reliable and economical safety assessment and design of ductile structures. Based on the elastic-perfectly plastic model of material, the theory of limit analysis has been developed since the early twentieth century. The analytical solution was originally reported by Gaydon *et al.* [1] for limit analysis of a square plate with a central circular. However, the analytical solution is not applicable to complex problems in engineering practice. Current research in the field of limit is focussing on the development of numerical tools which are sufficiently efficient and robust to overcome limitations of the analytical solution. Several numerical methods for limit analysis can be found in the literature such as Finite element method (FEM)**[**2], boundary element method (BEM) [3] and meshfree **[**4]. Based on the mentioned method, there are some approaches for limit analysis such as: upper bound solution, lower bound solution, mixed solution and so on. In practice, the limit analysis is mainly obtained by the finite element method, which is widely applied in engineering design. However, mesh generation based on discretizing geometry is required before analysis problem. This process takes 80% total time analysis. In order to overcome this difficulty, In recent years the IGA is introduced by Hughes *et al.* **[**5]. This method allows us to integrate the computer-aided geometric design (CAGD) representations directly into the element finite formulation. The isogeometric finite element formulation uses Non-uniform rational basis spline (NURBS) instead of the Lagrange interpolation in the FEM. The NURBS can provide higher continuity of derivatives in comparison with Lagrange interpolation functions. In addition, the order of the NURBS function can be easily elevated without changing the geometry or its parameterization [6].

In this paper, we present a formulation of the NURBS based on Bezier extraction in combining with SOCP for limit upper bound analysis of plane stress structures. The IGA solution can be improved using refinements. The efficiency and convergence of the method for limit analysis of plane stress structures are checked through several examples.

The paper is structured as follows: Section 2 describes a brief of the isogeometric analysis based on Bézier extraction. Isogeometric analysis procedure for limit analysis of structures is presented in Section 3. Section 4 presents several examples of the proposed approach. Finally, we close our paper with some concluding remarks.

2. NURBS BASED ON BÉZIER EXTRACTION FOR UPPER BOUND LIMIT ANALYSIS

2.1. Knot vector

Given a knot vector $\Xi = \{\xi_1, \xi_2, \cdots, \xi_{n+p+1}\}$ and the polynomial degree *p*, the B-spline basis functions are defined following Ref [5].

$$N_{1,0}(\xi) = \begin{cases} 1 \ \textit{if} \ \xi_i \le \xi < \xi_{i+1} \\ 0 \ \textit{otherwise} \end{cases} \quad \text{for } p = 0 \tag{1}$$

and for $p > 0$

$$N_{i,p}(\xi) = \frac{\xi - \xi_i}{\xi_{i+p} - \xi} N_{i,p-1}(\xi) + \frac{\xi_{i+p+1} - \xi}{\xi_{i+p+1} - \xi_{i+p}} N_{i+1,p-1}(\xi). \tag{2}$$

Due to being able to exactly represent the geometry, NURBS are widely used in computer-aided design (CAD). NURBS basis function can be obtained by including weights w_i to control points

$$R_i^p(\xi) = \frac{N_{i,p}(\xi) w_i}{\sum_{i=1}^{n} N_{i,p}(\xi) w_i} \tag{3}$$

The NURBS in two dimensional space can be obtained as tensor products of one-dimensional space as below:

$$R_{i,j}^{p,q}(\xi,\eta) = \frac{N_{i,p}(\xi) M_{j,q}(\eta) w_{i,j}}{\sum_{\hat{i}=1}^{n} \sum_{\hat{j}=1}^{m} N_{\hat{i},p}(\xi) M_{\hat{j},q}(\eta) w_{\hat{i},\hat{j}}} \tag{4}$$

The displacement field is expressed as

$$\boldsymbol{u}^h = \sum_{A=1}^{m \times n} \boldsymbol{R}_A(\xi,\eta) \boldsymbol{q}_A \tag{5}$$

where $\boldsymbol{q}_A$ is control point displacements associated with control point A. $\mathbf{R}_A(\xi,\eta) = R_{i,j}^{p,q}(\xi,\eta)$ is NURBS basis function in 2D.

Based on a set of original control points $\mathbf{P} = \{P_i\}_{i=1}^{n}$ of a B-spline curve, we can obtain *m* new control $\{\bar{P}_i\}_{i=1}^{m}$ followed the formulation

$$\bar{P}_i = \begin{cases} P_1 & i = 1 \\ \alpha_i P_i + (1-\alpha_i) P_{i-1} & 1 \le i \le m \\ P_n & i = m \end{cases} \tag{6}$$

where α_i defined as

$$\alpha_i = \begin{cases} 1_1 & 1 \le i \le k-p \\ \dfrac{\bar{\xi} - \xi_i}{\xi_{i+p} - \xi_i} & k-p+1 \le i \le k \\ 0 & i \ge k+1 \end{cases} \tag{7}$$

According to Ref [7], the Bézier extraction operator can be computed as below:

$$\mathbf{C}^j = \begin{bmatrix} \alpha_1 & 1-\alpha_2 & 0 & \cdots & & & 0 \\ 0 & \alpha_2 & 1-\alpha_3 & 0 & \cdots & & 0 \\ 0 & 0 & \alpha_3 & 1-\alpha_4 & 0 & \cdots & 0 \\ \vdots & & & & & & \\ 0 & \cdots & & & 0 & \alpha_{n+j-1} & 1-\alpha_{n+j} \end{bmatrix} \tag{8}$$

Eq (6) in matrix form can be expressed as

$$\bar{\mathbf{P}}^{j+1} = \left(\mathbf{C}^j\right)^T \bar{\mathbf{P}}^j \tag{9}$$

Defining $\mathbf{C}^T = \left(\mathbf{C}^m\right)^T \left(\mathbf{C}^{m-1}\right)^T \cdots \left(\mathbf{C}^1\right)^T$ we get the relation between new Bézier control points and original B-spline ones

$$\mathbf{P}^b = \mathbf{C}^T \mathbf{P} \tag{10}$$

where $\mathbf{C}$ is called the *Bezier extraction operator.*

Based on defining the curve, the B-spline basis functions and the Bernstein polynomials have relations as below:

$$\mathbf{N}^e(\xi) = \mathbf{C}^e \mathbf{B}_b(\xi) \tag{11}$$

where $\mathbf{N}^e(\xi), \mathbf{C}^e, \mathbf{B}_b(\xi)$ are B-spline basis functions, Bezier extraction operator and Bernstein basis functions of element *e*, respectively. The relation between the Bézier control points and the NUBRS control points can be obtained as follows

$$\mathbf{P}^b = \left(\mathbf{W}^b\right)^{-1} \mathbf{C}^T \mathbf{W}\mathbf{P} \tag{12}$$

where $\mathbf{W}^b$ is the Bézier weights.

The NURBS basis functions in Eq. (3) for element *e* using the Bézier extraction operator becomes

$$\mathbf{R}^e(\xi) = \frac{\mathbf{W}^e\mathbf{N}^e(\xi)}{W^b(\xi)} = \frac{\mathbf{W}^e\mathbf{C}^e\mathbf{B}^e(\xi)}{W^b(\xi)} \tag{13}$$

and Bézier extraction operator in 2D dimension

$$\mathbf{C}^e = \mathbf{C}^e(\xi) \otimes \mathbf{C}^e(\eta) \tag{14}$$

2.2. Kinematic formulation and solution procedure of the discrete problem

We consider a rigid-perfectly plastic body with boundary $\Gamma = \Gamma_t \cup \Gamma_u$ and $\Gamma_t \cap \Gamma_u = \emptyset$, where Γ_t is the static boundary and Γ_u is the kinematic boundary. The body is subjected to body forces f and surface tractions g on Γ_t. The constrained boundary Γ_u is fixed. According to the kinematic theorem, the collapse load multiplier λ^+ can be obtained by solving the following mathematical programming

$$\lambda^+ = \min D(\dot{\varepsilon}) \tag{15}$$

where strain rates $\dot{\varepsilon}$ is given by

$$\dot{\varepsilon} = [\dot{\varepsilon}_{xx} \quad \dot{\varepsilon}_{yy} \quad \dot{\varepsilon}_{xy}] = \sum_e \boldsymbol{B}_e \dot{\boldsymbol{u}}_e \tag{16}$$

$\boldsymbol{B}_e$ is the strain matrix given by

$$\boldsymbol{B}_e = \begin{bmatrix} \dfrac{\partial \boldsymbol{R}_e}{\partial x} & 0 & \dfrac{\partial \boldsymbol{R}_e}{\partial y} \\ 0 & \dfrac{\partial \boldsymbol{R}_e}{\partial y} & \dfrac{\partial \boldsymbol{R}_e}{\partial x} \end{bmatrix}^T \tag{17}$$

The plastic dissipation $D(\dot{\varepsilon})$ is defined by

$$D(\dot{\varepsilon}) = \underbrace{\max}_{\psi(\sigma)\le 0} \sigma : \dot{\varepsilon} \equiv \sigma_\varepsilon : \dot{\varepsilon} \tag{18}$$

where σ denotes the admissible stresses contained within the convex yield surface $\psi(\sigma)$ and σ_ε are the stresses on the yield surface associated with any strain rates ε through the plasticity condition. According to Ref [8], the plastic dissipation can be written as the function of strain rates

$$\begin{aligned} \mathrm{D}(\dot{\varepsilon}) &= \int_\Omega \sigma_0 \sqrt{\dot{\varepsilon}^T \Theta \dot{\varepsilon}}\, d\Omega \\ &= \sum_{e=1}^{nel} \int_{\Omega^e} \sigma_0 \sqrt{\dot{\varepsilon}^{eT} \Theta \dot{\varepsilon}^e}\, d\Omega^e \end{aligned} \tag{19}$$

where

$$\Theta = \frac{1}{3}\begin{bmatrix} 4 & 2 & 0 \\ 2 & 4 & 0 \\ 0 & 0 & 1 \end{bmatrix} \tag{20}$$

$\dot{\varepsilon}^e$ is plastic strains rate of element *e* and σ_0 is the yield stress. Eq. (19) computed at Gauss points over each element *e* becomes as follows:

$$\begin{aligned} D(\dot{\varepsilon}) &= \sum_{e=1}^{nel}\sum_{i=1}^{eGP} \sigma_0 \bar{w}_i |J_i| \sqrt{\dot{\varepsilon}_i^T \Theta \dot{\varepsilon}_i} \\ &= \sum_{i=1}^{nGP} \sigma_0 \bar{w}_i |J_i| \sqrt{\dot{\varepsilon}_i^T \Theta \dot{\varepsilon}_i} \end{aligned} \tag{21}$$

The Eq. (21) can be written in a form involving a sum of norms as

$$\begin{aligned} D(\dot{\varepsilon}) &= \sum_{i=1}^{nGP} \sigma_0 \bar{w}_i |J_i| \left\| \boldsymbol{C}_f^T \dot{\boldsymbol{\varepsilon}}_i \right\| \\ &= \sum_{i=1}^{nGP} \sigma_0 \bar{w}_i |J_i| \, \|\boldsymbol{\rho}_i\| \end{aligned} \tag{22}$$

where $\bar{w}_i$, $|J_i|$ and $\dot{\varepsilon}_i$ are the weight value, determinant of the Jacobian matrix and plastic strains rate at the Gauss point *i*, respectively. $nGP = nel \times eGP$ is the total number of the Gauss points of the problem. $\|.\|$ in the plastic dissipation function is the Euclidean norm, $\|\mathrm{v}\| = \sqrt{(\mathrm{v}^T\mathrm{v})}$ and $\boldsymbol{C}_f$ expressed in Eq. (23) denotes for Cholesky factor of Θ.

$$\boldsymbol{C}_f = \frac{1}{\sqrt{3}}\begin{bmatrix} 2 & 0 & 0 \\ 1 & \sqrt{3} & 0 \\ 0 & 0 & 1 \end{bmatrix} \tag{23}$$

and $\boldsymbol{\rho}_i = [\rho_1 \quad \rho_2 \quad \rho_3]^T = \boldsymbol{C}_f^T \dot{\boldsymbol{\varepsilon}}_i$ is a vector of additional variables to make the optimization problem in Eq. (15) become a problem of a sum of norms as

$$\lambda^+ = \min \sigma_0 \sum_{i=1}^{nGP} \overline{w}_i |J_i| \|\boldsymbol{\rho}_i\|$$

subjected to:

$$\begin{cases} \dot{\boldsymbol{u}} = 0 \qquad on\ \Gamma_u \\ \boldsymbol{\rho}_i = \boldsymbol{C}_f^T \dot{\boldsymbol{\varepsilon}}_i \\ \dot{\boldsymbol{\varepsilon}}_i = \sum_{i=1}^{nGP} \boldsymbol{B}_i^e \dot{\boldsymbol{u}}_e \\ W_{ex}(\dot{\boldsymbol{u}}) = 1 \end{cases} \tag{24}$$

In order to efficiently solve the limit analysis problem, we use the Mosek optimization package [9]. By introducing the new variables t_i, the problem in Eq. (24) becomes as follows

$$\lambda^+ = \min \sigma_0 \sum_{i=1}^{nGP} \overline{w}_i |J_i| t_i$$

subjected to:

$$\begin{cases} \dot{\boldsymbol{u}} = 0 \qquad on\ \Gamma_u \\ \|\boldsymbol{\rho}_i\| \le t_i \quad \forall i = 1{:}nGP \\ \boldsymbol{\rho}_i = \boldsymbol{C}_f^T \dot{\boldsymbol{\varepsilon}}_i \\ \dot{\boldsymbol{\varepsilon}}_i = \sum_{i=1}^{nGP} \boldsymbol{B}_i^e \dot{\boldsymbol{u}}_e \\ W_{ex}(\dot{\boldsymbol{u}}) = 1 \end{cases} \tag{25}$$

where the second constraint in Eq. (25) represents quadratic cones.

3. NUMERICAL VALIDATION

In this section, we illustrate some numerical examples to validate the present method. All numerical examples are considered in plane stress state and von Mises criterion.

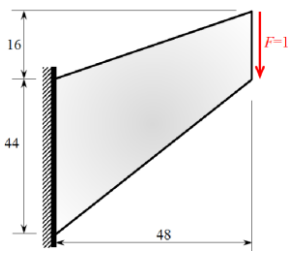

Fig 1. *Cook's problem model with boundary conditions and shear traction.*

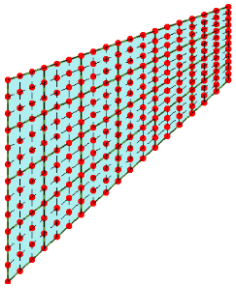

Fig 2. *Quartic NURBS mesh with 24 elements.*

3.1 Cook's Problem

The first example considered to validate our present approach is a Cook's problem, The boundary condition, applied load and geometry properties illustrate in Fig 1. The material data is assumed as: $E = 2.1\times10^5$ MPa, ν = 0.3 and $\sigma_0 = \sqrt{3}$ MPa.

Table 1. *The limit load factor of the present approach for the Cook's problem*

Authors & Methods	Mesh discretization		
	4x6	6x9	8x12
CS-FEM [10]		0.6852	
IGA-Bezier, SOCP ($p = 2$)	0.6930	0.6906	0.6878
IGA-Bezier, SOCP ($p = 3$)	0.6888	0.6854	0.6854
IGA-Bezier, SOCP ($p = 4$)	0.6883	0.6847	0.6850

The problem is discretized into 24 NURBS elements (494 degrees of freedom) as displayed in Fig 2. This problem is investigated by Canh V. Le [10], H. Ciria and J. Peraire [11]. The results of the present method are listed in Table 1. It can be obtained that our results are good agreements with the available reference.

3.2 Square plate with a central circular hole

The next example is a square plate with a central circular hole subjected to biaxial uniform loads P_1, P_2 as shown in Fig 3. This problem is a well-known benchmark, investigated by many researchers such as Belytschko [12], Zhang *et al.* [16], Nguyen *et al*[13] and so on. Due to the symmetry, a quarter of the problem is considered as

shown in Fig 4: Quadratic NURBS mesh with 16 elements. Fig 4 also illustrates the boundary condition and applied loads in a symmetry condition.

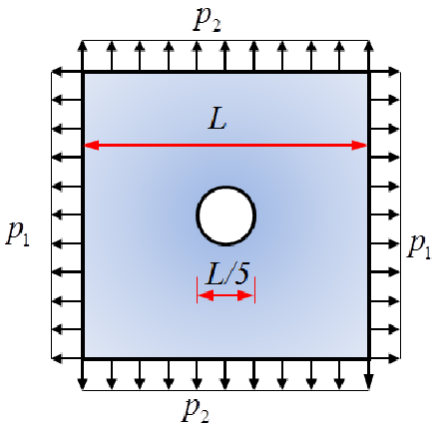

Fig 3. *The full model of the square plate with a central circular hole subjected two loads and boundary conditions.*

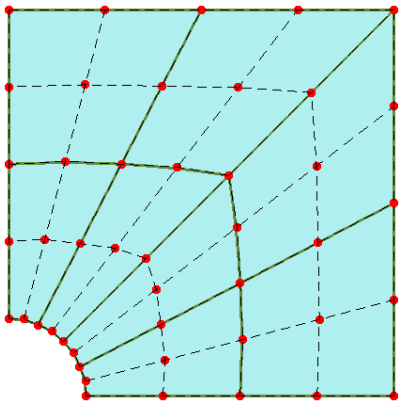

Fig 4. *Quadratic NURBS mesh with 16 elements.*

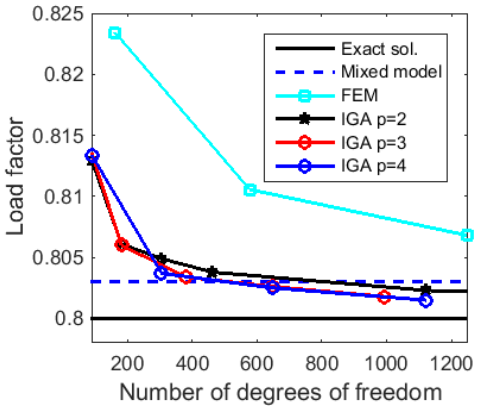

Fig 5. *The convergence of the present method compared with other solutions for the case $P_2 = 0$.*

The given data is assumed as $E = 2.1\times10^5$ MPa, $\nu = 0.3$ and $\sigma_0 = 200$ MPa. We discretize the problem domain into three NURBS meshes corresponding with 8, 32 and 128 elements, respectively. The results of this example are listed in Table 2, Table 3 compared with other available solutions in the literature. From Fig 5, it can be seen that our solution agrees very well with the other solutions such as FEM[12], BEM[16], EFG[14] and so on. Fig 5 shows the convergence of the present approach compared with other methods. It can be concluded that our results rapidly converge to the exact solution.

3.3 A symmetric continuous beam

The last example is considered as a symmetric continuous beam [18], subjected to two loads P_1 and P_2, as illustrated in Fig 6. Our study is carried out three meshes corresponding with 800, NURBS elements, respectively. The material parameters are assumed as follow E = 1.8×105 MPa, $\nu = 0.3$ and $\sigma_0 = 100$ MPa. The limit load values are listed in Table 4. The present results show good agreements with other methods.

Table 2. *The limit load factor of the present approach for the square plate with a central circular hole.*

Load cases	Polynomial order	Mesh discretization		
		2(2 × 2)	2(4 × 4)	2(8 × 8)
$P_2 = 0$	Quadratic	0.8130	0.8049	0.8023
	Cubic	0.8060	0.8026	0.8011
	Quartic	0.8037	0.8015	0.8011
$P_2 = \frac{P_1}{2}$	Quadratic	0.9213	0.9158	0.9136
	Cubic	0.9163	0.9130	0.9116
	Quartic	0.9143	0.9129	0.9113
$P_2 = P_1$	Quadratic	0.9024	0.8976	0.8966
	Cubic	0.8976	0.8961	0.8957
	Quartic	0.8963	0.8962	0.8955

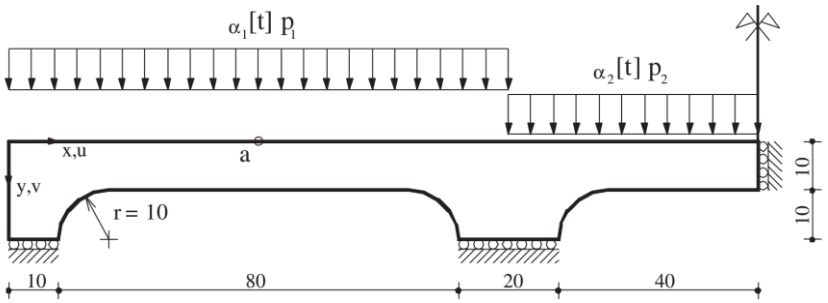

Fig 6. *Geometry of the symmetry continuous beam.*

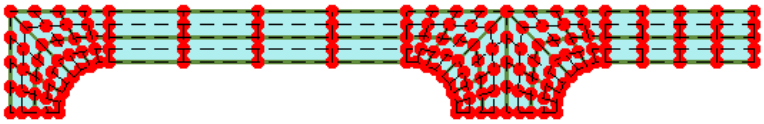

Fig 7. *A quadratic NURBS mesh with 32 elements and 165 number control points.*

Table 3. *The limit load factor of the IGA based on Bézier extraction for the square plate with a central circular hole in comparison with the other method.*

Approach & Method	Authors	Load cases		
		$P_2 = P_1$	$P_2 = P_1/2$	$P_2 = 0$
Present approach (UB)	Quadratic (*ndofs* = 462)	0.8969	0.9145	0.8038
	Cubic (*ndofs* = 650)	0.8961	0.9130	0.8026
	Quartic (*ndofs* = 650)	0.8955	0.9113	0.8025
Equilibrium FEM (LB)	Belytschko *et al.*[12]	---	---	0.78
Equilibrium FEM (LB)	Nguyen & Palgen[13]	0.704	---	0.564
EFG (LB)	Chen *et al.*[14]	0.874	0.899	0.798
Mixed model	Zouain *et al.*[15]	0.894	0.911	0.803
BEM (LB)	Zhang *et al.*[16]	0.889	0.898	0.784
NS-FEM (DA)	Nguyen *et al.*[17]	0.894	0.911	0.802
Analytical	Gaydon *et al.*[1]	0.894	--	0.8

LB (Lower bound); UB (Upper bound); DA (Dual algorithm); NS (Node smoothed)

Table 4. *The limit load factor of the continuous symmetric beam*

			Limit load factor		
		(P_1, P_2) [MPa]	(2, 0)	(0, 1)	(1.2, 1)	(2, 1)
Present approach (Upper bound)	Quadratic, *ndofs = 4386*		3.419	8.785	5.612	3.4670
	Cubic, *ndofs = 5510*		3.365	8.918	5.598	3.5288
	Quartic, *ndofs = 4386*		3.448	8.938	5.6689	3.395
Ref [18]			3.280	8.718	5.467	3.280
Hien *et al.* [19]	Quadratic		3.322	8.781	5.538	3.322
	Cubic		3.305	8.744	5.508	3.305
	Quartic		3.295	8.723	5.493	3.295

4. CONCLUSIONS

We have presented a new numerical approach for computing the limit load factor of plane stress problem in this paper by using the NURBS based on Bézier extraction in combination with the SOCP. Numerical examples are given to illustrate the accuracy and effectiveness of the present method in comparison with other method solutions. In the future, we continuous developing the present method to 2D plane strain and 3D problem with referring to incompressibility problem.

ACKNOWLEDGMENT

The first and second authors would like to thank HCMUTE for the support under the Grant No. TĐ2018-10TĐ.

REFERENCES

[1] F.A. Gaydon, A.W. McCrum, A theoretical investigation of the yield-point loading of a square plate with a central circular hole, *Journal of Mechanics and Physics of Solids*. 2, pp.156-169, 1954.

[2] A. Capsoni, L. Corradi, A finite element formulation of the rigid-plastic limit analysis problem, *International Journal for Numerical Methods in Engineering*. 40, pp. 2063-2086, 1997.

[3] Z. Zhang, Y. Liu, Z.Cen, Boundary element methods for lower bound limit and shakedown analysis, *International Journal for Numerical Methods in Engineering*. 191, pp. 905-917, 2004.

[4] S. Chen, Y. Liu, Z. Cen, Lower-bound limit analysis by using the EFG method and nonlinear programming. *International Journal for Numerical Methods in Engineering.* 74, pp.391-415, 2008.

[5] T.J.R. Hughes, J.A. Cottrell, Y. Bazilevs, Isogeometric analysis: CAD, finite elements, NURBS, exact geometry and mesh refinement, *Computer Methods in Applied Mechanics and Engineeering.* 194, pp.4135–4195, 2005.

[6] J. Cottrell, T.J.R. Hughes, A. Reali, Studies of refinement and continuity in isogemetric analysis, *Computer Methods in Applied Mechanics and Engineeering.* 196, pp. 4160–4183, 2007.

[7] Borden MJ, Scott MA, Evans JA, Hughes TJR. Isogeometric finite element data structures based on Bézier extraction of NURBS. *International Journal for Numerical Methods in Engineering.* 86, pp. 15 – 47, 2011.

[8] A. Capsoni, L. Corradi, A finite element formulation of the rigid-plastic limit analysis problem, *International Journal for Numerical Methods in Engineering.* 40, pp. 2063–2086, 1997.

[9] Mosek, The MOSEK Optimization Toolbox for MATLAB Manual. Mosek ApS, version 5.0 ed., 2009. <http://www.mosek.com>.

[10] Le CV, Nguyen-Xuan H, Askes H, Bordas S, Rabczuk T, Nguyen-Vinh H. A cell-based smoothed finite element method for kinematic limit analysis, *International Journal for Numerical Methods in Engineering.* 88(12), pp.1651–1674, 2010.

[11] H. Ciria, J. Peraire, J. Bonet , Mesh adaptive computation of upper and lower bounds in limit analysis, *International Journal for Numerical Methods in Engineering.*75(8), pp.899–944, 2008.

[12] Belytschko T, Plane stress shakedown analysis by finite elements, *International Journal Mechanical Science*.14, pp.619–625, 1972.

[13] Nguyen DH, Palgen L. Shakedown analysis by displacement method and equilibrium finite elements. Proceedings of SMIRT-*5*, Berlin1 979;p L3/3.

[14] Chen S, Liu Y, Cen Z, Lower-bound limit analysis by using the EFG method and non-linear programming. *International Journal for Numerical Methods in Engineering.* 74, pp.391-4157, 2008.
[15] Zouain Z, Borges L, Silveira JL, An algorithm for shakedown analysis with nonlinear yield functions, *Computer Methods in Applied Mechanics and Engineeering.* 191, pp.2463–2481, 2002.
[16] Zhang Z, Liu Y, Cen Z, Boundary element methods for lower bound limit and shakedown analysis, *Engineering Analysis with Boundary Elements*. 28, pp.905–917, 2004.
[17] H. Nguyen-Xuan, T. Rabczuk, T. Nguyen-Thoi, T. N. Tran, N. Nguyen-Thanh. Computation of limit and shakedown loads using a node-based smoothed finite element method, *International Journal for Numerical Methods in Engineering.* 90, pp.287 – 310, 2012.
[18] Garcea G, Armentano G, Petrolo S, Casciaro R, Finite element shakedown analysis of two-dimensional structures. *International Journal for Numerical Methods in Engineering.* 63, pp.1174–1202, 2005.
[19] Hien V. Do, H. Nguyen-Xuan, Limit and shakedown isogeometric analysis of structures based on Bézier extraction, *European Journal of Mechanics / A Solids. 63, pp. 149-164, 2017.*

Corresponding author:
Do Van Hien
Ho Chi Minh City University of Technology and Education
Email: hiendv@hcmute.edu.vn